Structure−Activity Relationship Studies on a Series of Novel, Substituted 1-Benzyl-5-phenyltetrazole P2X7 Antagonists

Derek W. Nelson,* Robert J. Gregg, Michael E. Kort, Arturo Perez-Medrano, Eric A. Voight, Ying Wang, George Grayson, Marian T. Namovic, Diana L. Donnelly-Roberts, Wende Niforatos, Prisca Honore, Michael F. Jarvis, Connie R. Faltynek, and William A. Carroll

Abbott Laboratories, Neuroscience Research, Global Pharmaceutical Research and Development, Abbott Park, Illinois 60064-6101

1-Benzyl-5-aryltetrazoles were discovered to be novel antagonists for the P2X7 receptor. Structure−activity relationship (SAR) studies were conducted around both the benzyl and phenyl moieties. In addition, the importance of the regiochemical substitution on the tetrazole was examined. Compounds were evaluated for activity to inhibit calcium flux in both human and rat recombinant P2X7 cell lines using fluorometric imaging plate reader technology. Analogues were also assayed for their ability to inhibit IL-1β release and to inhibit P2X7-mediated pore formation in human THP-1 cells. Compound **15d** was advanced to efficacy studies in a model of neuropathic pain where significant reversal of mechanical allodynia was observed at doses that did not affect motor coordination.

Introduction

The P2X family of nucleotide receptors consists of nonspecific, ligand-gated cation channels that participate in a variety of physiological processes.[1−4] The homomeric subtype P2X7, formerly characterized as the P2Z receptor,[5,6] possesses a large extracellular loop, two transmembrane domains, a short intracellular *N*-terminus, and a long intracellular C-terminus.[7−9] P2X7 is expressed in the periphery on cells of the immune system such as macrophages and epidermal Langerhans cells.[6] The receptor is also expressed in the central nervous system on microglia[10] and astrocytes,[11] although the presence of P2X7 on neurons remains controversial.[12] Brief activation of P2X7 by extracellular ATP initiates a complex sequence of events, including ion influx,[13] caspase-1 activation,[14] release of the proinflammatory cytokine IL-1β,[15,16] and p38 MAP kinase activation.[17] Prolonged activation results in reversible cell membrane pore formation, leading to lysis and cell death.[4] P2X7 receptor activation has also been linked to glutamate release and inhibition of glutamate uptake.[18]

Due to the presence of the P2X7 receptor on cells of the immune system (macrophages, microglia, etc.) and the relationship between P2X7 activation and cytokine or glutamate release, this receptor may play an important role in the development and progression of various disease states or conditions such as chronic inflammation,[19] neurodegeneration,[20] and chronic pain.[21] Particularly intriguing is the gathering body of literature linking activated microglia and astrocytes to central sensitization and the development and maintainence of neuropathic pain.[21−25] More direct evidence for the role of P2X7 in the development of inflammation and pain comes from experiments using P2X7-deficient mice.[26] In an anti-collagen arthritis model, knock-out (KO) animals showed a substantial reduction in symptom severity relative to wild-type controls.[26a] KO mice were also protected from the development of both adjuvant-induced inflammatory pain and partial nerve ligation induced neuropathic pain.[26b] Recent in vivo pharmacological studies have also pointed to the potential benefit of P2X7 antagonism in the treatment of spinal cord injury[20d] and chronic pain.[27]
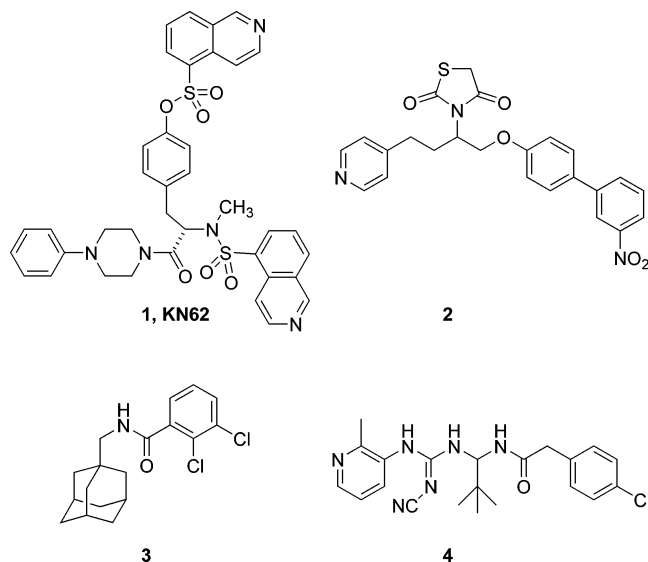

Figure 1.

Despite the potential therapeutic applications, few druglike P2X7 antagonists have appeared in the literature. KN-62 (**1**) (Figure 1) was the first small molecule antagonist to be identified[28] and it has been the starting point for several extensive SAR studies.[29] Two representative examples of novel chemotypes that have recently been disclosed with potent in vitro activity are compounds **2**[30] and **3**.[31] From our own laboratories, the cyanoguanidine-containing compound **4** (A-759020) was found to have potent activity in vitro against P2X7 and was also active in in vivo pain models.[32] A high-throughput screen (HTS) of our corporate compound library revealed the disubstituted tetrazole **5** (Figure 2) as a novel P2X7 antagonist (pIC50 = 6.9) in the recombinant human cell line. The low molecular weight of compound **5** and potential for chemical modification make it an attractive starting point for the optimization of potency as well as physiochemical and pharmacokinetic properties. We describe herein SAR studies around **5** that delineate the key substitutions influencing potency at P2X7 with this pharmacophore. In addition, we have identified

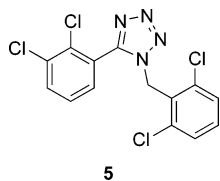* Corresponding author. Tel: (847) 937-9825. Fax: (847) 935-5466. E-mail: derek.nelson@abbott.com.

5

Figure 2.

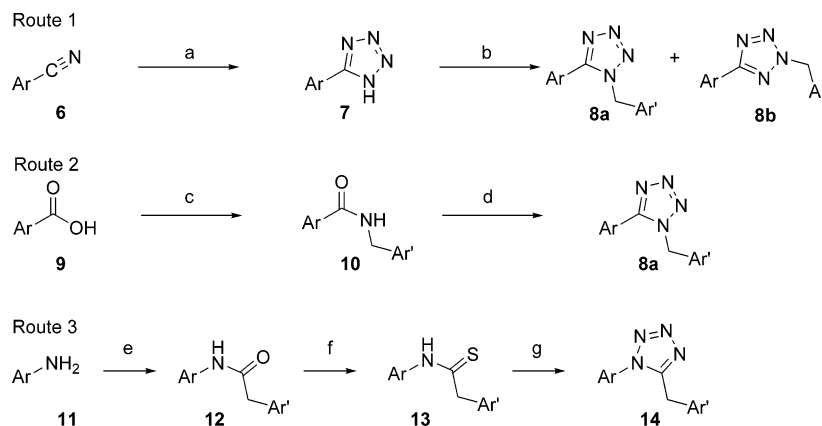compound **15d** as a representative example that exhibits efficacy in a behavioral model of neuropathic pain.

Chemistry

Initial SAR studies targeted the two phenyl rings of structure **5**. Analogues were synthesized by one of the sequences shown in Scheme 1. The tetrazole ring could be established by cycloaddition of azide with benzonitrile derivatives (**6**).[33] Subsequent benzylation of the 5-aryl *N*-H tetrazole (**7**) afforded a separable mixture of regioisomeric tetrazoles containing the desired 1,5-disubstituted product (**8a**) as the minor component (Scheme 1, route 1).[34] An alternate sequence for tetrazole formation involved conversion of an amide (**10**) to only the desired regioisomer (**8a**) using Mitsunobu conditions (Scheme 1, route 2).[35] The Mitsunobu method worked with amides derived from benzoic acids (**9**) but not with amides derived from arylacetic acids (**12**). A general synthetic approach to tetrazoles with reversed connectivity for the phenyl and benzyl moieties involved conversion of the amide (**12**) to the corresponding thioamide (**13**) followed by treatment with mercury(II) salts in the presence of trimethylsilyl azide to form the tetrazole (**14**) (Scheme 1, route 3).[36]

Biology

In Vitro. Functional P2X$_7$ activity was measured using three different methods: (1) inhibition of Ca^{2+} flux in recombinant human or rat cell lines, (2) inhibition of IL-1β release in human THP-1 cells, and (3) blockade of pore formation in human THP-1 cells. Inhibition of Ca^{2+} flux was measured with a fluorometric imaging plate reader (FLIPR) using Fluo-4 as the calcium-sensing dye and benzoylbenzoylATP (BzATP) as the agonist.[37] The FLIPR experiments utilized a 5-min pretreatment with the antagonist. Increased pretreatment times of 15, 30, and 60 min resulted in no change in the measured IC$_{50}$ values. The recombinant human and rat P2X$_7$ were functionally expressed in stably transfected human 1321N1 astrocytoma cells devoid of endogenous P2X receptor function. An inhibition assay of IL-1β release was established in human THP-1 cells that had

Table 1. Functional Potency of Tetrazole P2X$_7$ Antagonists with Modified Benzylic Groups

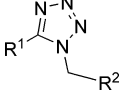| compd	R	pIC$_{50}$[a] hP2X$_7$ Ca^{2+} flux[c]	hYO-PRO[d]
15a	C$_6$H$_5$	7.4 ± 0.5	6.3 ± 0.1
15b	2-CH$_3$-C$_6$H$_4$	7.8 ± 0.5	6.9 ± 0.1
15c	2-pyridyl	6.3 ± 0.4[b]	5.7 ± 0.1
15d	3-pyridyl	6.9 ± 0.2	6.7 ± 0.1
15e	4-pyridyl	6.1 ± 0.1[b]	5.7 ± 0.1
15f	2-CH$_3$-3-pyridyl	7.5 ± 0.2	6.7 ± 0.1
15g	3-pyridinylmethyl	4.9 ± 0.2[b]	<5[b]
15h	2,4-(CH$_3$)$_2$-5-thiazolyl	7.3 ± 0.2	6.6 ± 0.1
15i	3,5-(CH$_3$)$_2$-4-isoxazolyl	6.8 ± 0.3	6.1 ± 0.2
3	−	7.2 ± 0.1	NT

a Number of determinations ≥ 3 unless otherwise indicated. *b* Number of determinations = 2. *c* Standard deviation shown. *d* Standard error shown. NT = not tested.

been differentiated with LPS and IFNγ then stimulated with BzATP for 30 min in the presence of test compounds.[17] Measurement of IL-1β release was performed using commercially available EIA kits. Finally, blockade of pore formation by test compounds was assessed by the YO-PRO uptake assay measuring the inhibition of cellular uptake of the impermeable YO-PRO-1 diiodide dye using differentiated human THP-1 cells stimulated with the agonist BzATP for 1 h.[17]

In Vivo. Efficacy in the reduction of neuropathic pain was evaluated using the L5/L6 spinal nerve tight ligation (Chung) model.[38] In these experiments, spinal nerve ligation was performed 7−14 days prior to assay. Tactile allodynia was induced by application of a von Frey hair 30 min after administration of the antagonist. Reduction in tactile allodynia was measured by determination of the paw withdrawal threshold and comparison to the contralateral paw. Potential motor impairment in test animals subjected to compounds was evaluated using the rotarod assay. Coordination was measured using an accelerating rotorod apparatus with the time required for the animal to fall from the rod being recorded.

Result and Discussion

Initial SAR studies focused on modification of the benzylic moiety to incorporate substituted phenyl groups or heterocycles (Table 1). Tetrazoles containing the benzyl group or a 2-sub-

Scheme 1[a]

a Conditions: (a) AlMe$_3$, TMSN$_3$, toluene, Δ; (b) ClCH$_2$Ar′ or BrCH$_2$Ar′, NEt$_3$, CH$_3$CN, rt; (c) SOCl$_2$, DMF, toluene, Δ then H$_2$NCH$_2$Ar′; (d) DIAD, PPh$_3$, TMSN$_3$, THF, rt; (e) ClCOCH$_2$Ar′, NEt$_3$, THF; (f) Lawesson's reagent, toluene, Δ; (g) Hg(OAc)$_2$, TMSN$_3$, NEt$_3$, THF, 0 °C.

Table 2. Functional Potency of Tetrazole P2X$_7$ Antagonists with Modified Phenyl Groups

compd	R^1	R^2	hP2X$_7$ Ca^{2+} flux^c	hYO-PRO^d
16a	C$_6$H$_5$	3-pyridyl	4.6 ± 0.4^b	<5^b
16b	2-Cl-C$_6$H$_4$	3-pyridyl	4.8 ± 0.1^b	NT
16c	3-Cl-C$_6$H$_4$	3-pyridyl	5.1 ± 0.3	<5^b
16d	2,5-Cl$_2$-C$_6$H$_3$	3-pyridyl	4.8 ± 0.7^b	<5^b
16e	3,4-Cl$_2$-C$_6$H$_3$	3-pyridyl	5.4 ± 0.3	5.1 ± 0.1
16f	2,3-(CH$_3$)$_2$-C$_6$H$_3$	2-CH$_3$-C$_6$H$_4$	6.6 ± 0.4	5.9 ± 0.2
16g	2,3-(OCH$_3$)$_2$-C$_6$H$_3$	2-Cl-C$_6$H$_4$	5.4 ± 0.2^b	<5^b
16h	4-pyridyl	C$_6$H$_5$	4.5 ± 0.42^b	NT
16i	5-quinolyl	C$_6$H$_5$	4.8 ± 0.2	<5^b
16j	8-quinolyl	C$_6$H$_5$	4.6 ± 0.1^b	
16k	2,3-Cl$_2$-4-pyrrolidinyl-C$_6$H$_2$	C$_6$H$_5$	<5^b	NT
16l	2-CF$_3$-3-F-C$_6$H$_3$	3-pyridyl	6.2 ± 0.2^b	NT
16m	2-Cl-3-CF$_3$-C$_6$H$_3$	3-pyridyl	7.9 ± 0.2	6.8 ± 0.1
16n	2-F-3-CF$_3$-C$_6$H$_3$	3-pyridyl	7.2 ± 0.4	6.3 ± 0.4
16o	2,3-Cl$_2$-4-F-C$_6$H$_2$	3-pyridyl	7.9 ± 0.2	6.4 ± 0.1
16p	2,3,4-Cl$_3$-C$_6$H$_2$	3-pyridyl	6.7 ± 0.3	5.87 ± 0.1

^{a} Number of determinations ≥ 3 unless otherwise indicated. ^{b} Number of determinations = 2. ^{c} Standard deviation shown. ^{d} Standard error shown. NT = not tested.

Table 3. Functional Potency of Tetrazole P2X$_7$ Antagonists with Reversed Connectivity

compd	R^1	hP2X$_7$ Ca^{2+} flux^c	hYO-PRO^d
17a	2,3-Cl$_2$-C$_6$H$_3$	7.0 ± 0.2	6.4 ± 0.1
17b	2,3-Cl$_2$-4-F-C$_6$H$_2$	7.6 ± 0.4	NT
17c	2-Cl-3-CF$_3$-C$_6$H$_3$	7.9 ± 0.1	7.3 ± 0.1
17d	2-Cl-3-CF$_3$-4-F-C$_6$H$_2$	7.7 ± 0.2	6.8 ± 0.1

^{a} Number of determinations ≥ 3 unless otherwise indicated. ^{b} Number of determinations = 2. ^{c} Standard deviation shown. ^{d} Standard error shown. NT = not tested.

**Table 4.** Functional Potency of Tetrazole P2X$_7$ Antagonists against the Rat P2X$_7$ Receptor and in the Inhibition of Human IL-1β Release

compd	rP2X$_7$ Ca^{2+} flux^c	hIL-1β release	compd	rP2X$_7$ Ca^{2+} flux^c	hIL-1β release
15a	7.1 ± 0.4	5.6 ± 0.4	**15h**	5.9 ± 0.2^b	NT
15b	7.2 ± 0.5	6.8 ± 0.3	**16m**	7.2 ± 0.1	7.1 ± 0.2
15d	6.5 ± 0.2	6.4 ± 0.3	**16n**	7.1 ± 0.1	6.3 ± 0.1
15e	5.5 ± 0.1	4.7 ± 0.7^b	**17b**	7.0 ± 0.2	7.4 ± 0.4^b
15f	6.7 ± 0.2	6.8 ± 0.3	**17c**	7.3 ± 0.1	7.6 ± 0.1^b

^{a} Number of determinations ≥ 3 unless otherwise indicated. ^{b} Number of determinations = 2. ^{c} Standard deviation shown. NT = not tested.

stituted benzylic group exhibited good potency (**15a,b**). The limited solubility of such analogues in a suitable vehicle, however, prevented a definitive assessment of their pharmacokinetic properties, so attention was turned toward modifications that could impart greater aqueous solubility. Incorporation of a basic nitrogen into the benzylic moiety substantially decreased antagonist potency for compounds **15c** and **15e** on the basis of the calcium influx and pore formation assays. Compound **15d** containing the pyridine attached at the 3-position, however, exhibited superior potency in both functional assays to **15c** and **15e**. Compound **15f**, bearing a methyl group at the 2-position, possessed 4-fold improved potency in the Ca^{2+} flux assay but not in the pore formation assay. Elongation of the spacer between the tetrazole and the pyridyl group significantly decreased antagonist potency (**15g**). Heterocycles that maintained a nitrogen in an orientation similar to that of the 3-pyridyl nitrogen (**15h,i**) afforded comparable potency in the calcium influx assay to **15d**, but potency in the pore formation assay decreased. Finally, the 2,5-regioisomer **8b** generated as the major product in route 1 (Scheme 1) was found to be completely inactive at P2X$_7$ (data not shown).

After the SAR studies involving modification of the benzylic group, optimization of the aromatic moiety bound directly to the tetrazole core was undertaken (Table 2). It was found that significant change to the substitution pattern of this region was not well tolerated. For example, the unsubstituted and monochloro derivatives **16a–c** were substantially less potent than compound **15d**. Likewise, both 2,5- and 3,4-dichloro variations (**16d,e**) lost 30–100-fold in potency relative to **15d**. Other 2,3-disubstituted phenyl moieties with methyl or methoxy groups decreased antagonist activity (**16f,g**). Heterocycles and amine substituents also caused a substantial loss of antagonist potency (**16h–k**). On the other hand, conservative modifications such as selective replacement of the 3-chloro substituent with a trifluoromethyl group generated more potent antagonists (**16m,n**). Addition of halogens at C(4) of the phenyl ring to establish trisubstituted benzene derivatives provided variable results, with fluorine increasing potency in the calcium-flux assay but not in the YO-PRO assay (**16o**) and chlorine having little effect on

potency (**16p**). Although the favorable 2,3-dichloro substitution pattern of analogues such as **15d** is the same as that on the aromatic ring of adamantylamide **3**, it is unclear at present if both of these molecules are binding in the same orientation with respect to the 2,3-dichlorophenyl. The published SAR around compound **3** certainly indicates a much greater latitude for modification of the phenyl substitution with retention of P2X$_7$ activity compared to the tetrazole analogues described here.[31]

Several tetrazoles in which the phenyl group was bound to the tetrazole moiety at N(1) and the benzylic moiety at C(5) were synthesized and evaluated in the in vitro assays (Table 3). The reversal of connectivity in the tetrazole pharmacophore (**17a–d** vs **15d**, **16m,o**) had little effect on potency in the calcium influx FLIPR assay. An improvement in potency in the YO-PRO assay was observed for the reverse tetrazole bearing the 2-chloro-3-trifluoromethylphenyl moiety (**17c** vs **16m**).

Selected tetrazole antagonists were also evaluated at the recombinant rat P2X$_7$ receptor and for their ability to inhibit IL-1β release in human THP-1 cells (Table 4). Generally, the tetrazoles demonstrated greater potency (~3-fold) at the human P2X$_7$ receptor compared to rat P2X$_7$ in the calcium influx assay, although the rank order potencies in the two assays were qualitatively similar (Figure 3). Species differences can range substantially higher, as indicated by the 20-fold difference in potencies at rat and human P2X$_7$ observed for compound **15h**. The compounds in Table 4 effectively inhibited IL-1β release with potencies that were less than those in the Ca^{2+} flux assay (Figure 4). Reduced potency was also observed in the pore formation assay relative to Ca^{2+} flux (Figure 5), although the magnitude of the effect was less than for the IL-1β assay. Differences in cell lines, times of exposure to the antagonist, and the sequences of the signaling events measured in the three different readouts of human P2X$_7$ function may contribute to the discrepancies, but the same rank order potencies were
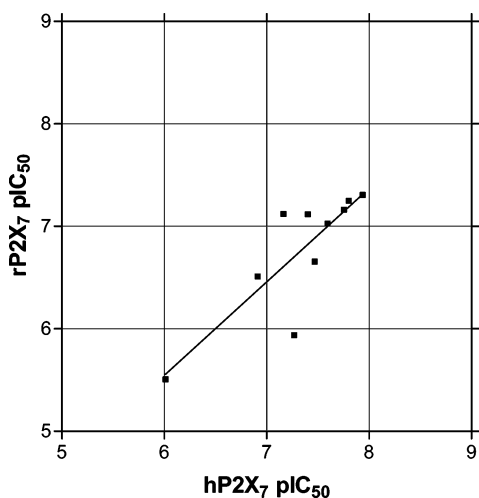
Figure 3. Comparison of human and rat $P2X_7$ potency. Slope $= 0.91$; $R^2 = 0.70$.
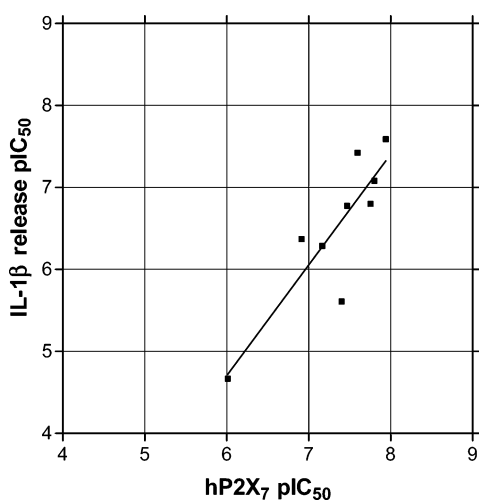
Figure 4. Comparison of potency to inhibit Ca^{2+} flux and IL-1β release. Slope $= 1.35$; $R^2 = 0.76$.
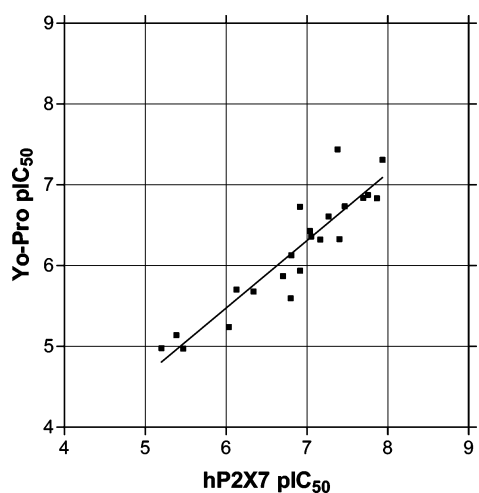
Figure 5. Comparison of potency to inhibit Ca^{2+} flux and pore formation. Slope $= 0.84$; $R^2 = 0.84$.

observed in all three. Although the relationship between inhibition of IL-1β release and potential antiinflammatory effects of a $P2X_7$ antagonist is evident, in the context of chronic or neuropathic pain it is presently unclear which of the three in vitro assays utilized in this study would be of greater relevance.

As a representative early example from this series, compound **15d** was evaluated for selectivity at other P2 receptors ($P2X_3$, $P2X_4$, and $P2Y_2$), where it was not found to have any significant interactions up to 10 μM. Compound **15d** was found to right-shift the agonist dose−response curve for BzATP at the human $P2X_7$ receptor in the FLIPR assay (Figure 6). A Schild analysis of these data generate a pA_2 of 6.9 (slope $= 0.87 \pm 0.14$). The FLIPR data used in the Schild analysis may not arise from a system at equilibrium, but control experiments in which the time of the FLIPR response after pretreatment with **15d** was varied from 3 to 60 min showed no shift in the dose response curve. As a result, the Schild analysis shown in Figure 6 is consistent with competitive antagonism by **15d**. In electrophysiology studies, **15d** similarly inhibited BzATP-evoked current (pIC_{50} $\sim$ 6.6) at the human $P2X_7$ receptor (Figure 7). The BzATP-induced currents were restored following washout of **15d**. Given its selectivity for $P2X_7$, compound **15d** represented an attractive tool with which to probe the behavorial effects of this pharmacology in the spinal nerve ligation (Chung) model of neuropathic pain in rats. Intraperitoneal (ip) administration of **15d** (10−300 μmol/kg) resulted in a dose-dependent reversal of mechanical allodynia on the injured (left) side with an ED_{50} value of 76 μmol/kg and a maximal response of 78% relative to the contralateral (noninjured) side (Figure 8). No behavorial effect was observed on the contralateral side. Consistent with these behavioral results, compound **15d** showed 19% bioavailability (ip) and a 1 h half-life in separate pharmacokinetic studies.[39] Evaluation of the effects of compound **15d** on motor coordination was also assessed using the rotarod assay. Up to doses of 300 μmol/kg (ip), **15d** failed to show a significant impairment of motor function (data not shown).

Conclusion

We have identified a novel tetrazole-based series of small molecule $P2X_7$ antagonists that shows potency comparable to that of known $P2X_7$ antagonists. The SAR studies conducted on the phenyl and benzyl moieties established the preferred substituents for $P2X_7$ activity in both these regions. In general, significant structural variation was not well tolerated on the phenyl group. However, modification of the benzylic moiety, particularly the incorporation of certain heterocycles, could impart a favorable balance of potency and physiochemical properties to allow for further in vivo evaluation. The three different in vitro assays utilized in this study represent different stages of the $P2X_7$ signaling cascade, yet the rank order potencies for compounds from this series were largely the same. Some species differences in potency for rat versus human $P2X_7$ were noted in this series, a potential limitation in selecting analogues for in vivo evaluation. A Schild analysis using FLIPR data to monitor calcium influx suggests competitive displacement of agonist BzATP, which distinguishes **15d** from noncompetitive antagonists such as KN62. Finally, compound **15d** was found to possess antinociceptive activity in a model of neuropathic pain, providing additional evidence for the potential of $P2X_7$ as a novel target for pain.

Experimental Section

Chemistry. General. Proton NMR spectra were obtained on a General Electric QE 300 or QZ 300 MHz instrument with chemical shifts (δ) reported relative to tetramethylsilane as internal standard. Mass spectral data were obtained using an electrospray (ESI) technique or by direct chemical ionization (DCI) methods employing ammonia. Elemental analyses were performed by Robertson Microlit Laboratories. Column chromatography was carried out on silica gel (230−400 mesh). Thin-layer chromatography (TLC) was
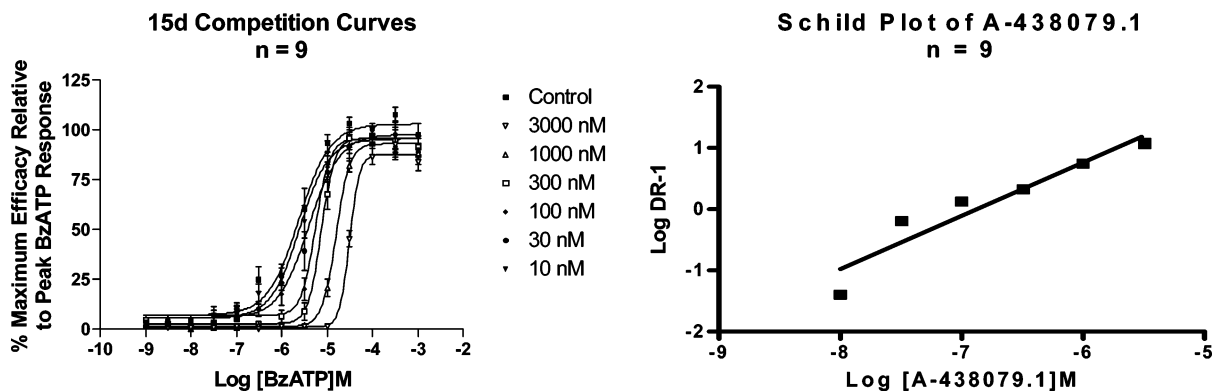
Figure 6. (A) Effects of compound **15d** to displace (parallel right-shift) the BzATP dose−response over the concentration range of 10−3000 nM. (B) Schild analysis for compound **15d**. Slope = 0.87 ± 0.14, pA_2 = 6.88.
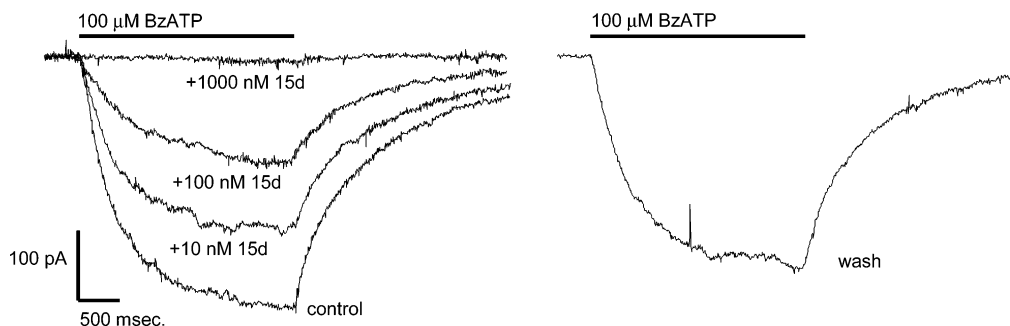
Figure 7. Concentration-dependent inhibition of BzATP-evoked current in hP2X$_7$ stable 1321N1 cells by **15d**. Representative current traces illustrating inhibition of 100 μM BzATP-evoked current by 10, 100, and 1000 nM **15d**. BzATP-evoked current amplitude after complete inhibition by antagonist (1 μM) returned to >85% of control following approximately 2 min of antagonist washout.
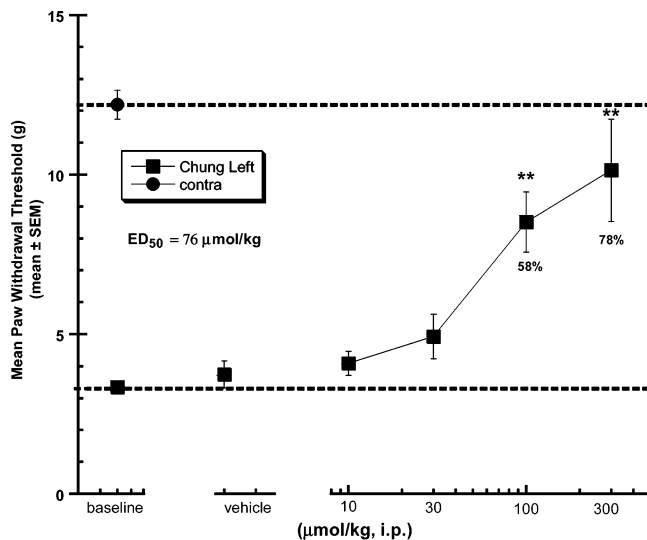
Figure 8. Effects of **15d** on mechanical allodynia observed in the Chung model of neuropathic pain.

performed using 250-mm silica gel 60 glass-backed plates with F$_{254}$ as indicator. LC−MS analyses were performed on ThermoQuest Navigator systems using 10−100% acetonitrile:10 mM ammonium acetate gradient with MS data obtained using atmospheric pressure chemical ionization (APCI) positive ionization over the range of *m/z* from 170 to 1200.

Representative Procedure for Tetrazole Alkylation (Route 1, Step b). 3-[5-(2,3-Dichlorophenyl)tetrazol-1-ylmethyl]pyridine (15d). To an oven-dried, round-bottomed flask under dry nitrogen atmosphere were added 5-(2,3-dichloro-phenyl)-1*H*-tetrazole (2.0 g, 9.3 mmol) and 3-bromomethylpyridine hydrobromide (2.3 g, 9.3 mmol). The flask was sealed with a rubber septum. Anhydrous acetonitrile (20 mL) was added via syringe to form a white slurry. Triethylamine (3.2 mL, 2.3 g, 23 mmol) was added via syringe,

and the mixture was stirred at room temperature for 24 h. The reaction was monitored by TLC (silica gel/1:1 ethyl acetate:hexanes; 2,5-disubstituted product R_f = 0.4, 1,5-disubstituted product R_f = 0.3). Brine (15 mL) was added to quench the reaction and the mixture was transferred to a separatory funnel and then extracted with ethyl acetate. The combined organic extracts were dried over sodium sulfate, filtered, and concentrated by rotary evaporator. The regioisomeric disubstituted tetrazoles were separated by flash chromatography (TLC conditions) to give 540 mg (19%) of the desired 1,5-disubstitued tetrazole as a white powder.

The hydrochloride salt was prepared by treatment of the free base with excess etheric hydrogen chloride followed by removal of the solvent/volatiles by rotary evaporator. The salt was recrystallized from ethyl acetate/hexanes.

1-(2,6-Dichlorobenzyl)-5-(2,3-dichlorophenyl)-1*H*-tetrazole (5): ^{1}H NMR (DMSO-d_6) δ 7.94 (dd, *J* = 8.1, 1.7 Hz, 1H), 7.90 (dd, *J* = 7.8, 1.7 Hz, 1H), 7.56 (t, *J* = 8.0 Hz, 1H), 7.51−7.38 (m, 3H), 5.77 (s, 2H); MS (DCI/NH$_3$) *m/z* 375 (M + H)$^+$.

1-Benzyl-5-(2,3-Dichlorophenyl)-1*H*-tetrazole (15a): ^{1}H NMR (DMSO-d_6) δ 7.90 (dd, *J* = 7.7, 2.2 Hz, 1H), 7.60−7.50 (m, 2H), 7.31−7.23 (m, 3H), 7.08−7.00 (m, 2H), 5.56 (s, 2H); MS (DCI/NH$_3$) *m/z* 305 (M + H)$^+$. Anal. (C$_{14}$H$_{10}$Cl$_2$N$_4$) C, H, N.

5-(2,3-Dichlorophenyl)-1-(2-methylbenzyl)-1*H*-tetrazole (15b): ^{1}H NMR (DMSO-d_6) δ 7.89 (dd, *J* = 7.8, 1.7 Hz, 1H), 7.61 (dd, 1H, *J* = 7.8, 1.7 Hz, 1H), 7.53 (t, *J* = 7.8 Hz, 1H), 7.22−7.11 (m, 2H), 7.01 (td, *J* = 7.5, 1.7 Hz, 1H), 6.75 (d, 1H, *J* = 7.5 Hz, 1H), 5.6 (s, 2H), 2.08 (s, 3H); MS (DCI/NH$_3$) *m/z* 319 (M + H)$^+$. Anal. (C$_{15}$H$_{12}$Cl$_2$N$_4$) C, H, N.

2-[5-(2,3-Dichlorophenyl)tetrazol-1-ylmethyl]pyridine hydrochloride (15c): ^{1}H NMR (DMSO-d_6) δ 8.45 (ddd, *J* = 4.9, 1.5, 0.9 Hz, 1H), 7.89 (dd, *J* = 8.3, 1.5 Hz, 1H), 7.81 (td, *J* = 7.7, 1.8 Hz, 1H), 7.62 (dd, *J* = 7.7, 1.5 Hz, 1H), 7.52 (t, *J* = 7.8 Hz, 1H), 7.38−7.30 (m, 2H), 5.76 (s, 2H); MS (DCI/NH$_3$) *m/z* 306 (M + H)$^+$. Anal. (C$_{13}$H$_9$Cl$_2$N$_5$·HCl) C, H, N.

3-[5-(2,3-Dichlorophenyl)tetrazol-1-ylmethyl]pyridine hydrochloride (15d): ^{1}H NMR (DMSO-d_6) δ 8.70 (dd, *J* = 5.1, 1.4 Hz, 1H), 8.57 (d, *J* = 2.0 Hz, 1H), 7.99−7.92 (m, 2H), 7.72−7.56 (m,

3H), 5.74 (s, 2H); MS (DCI/NH$_3$) m/z 306 (M + H)$^+$. Anal.(C$_{13}$H$_9$-Cl$_2$N$_5$·HCl) C, H, N.

4-[5-(2,3-Dichlorophenyl)tetrazol-1-ylmethyl]pyridine hydrochloride (15e): ^{1}H NMR (DMSO-d_6) δ 8.66 (d, J = 6.1 Hz, 2H), 7.94 (dd, J = 8.1, 1.7 Hz, 1H), 7.66 (dd, 1H, J = 7.8, 1.7 Hz, 1H), 7.57 (t, J = 8.0 Hz, 1H), 7.37 (d, J = 6.1 Hz, 2H), 5.80 (s, 2H). Anal. (C$_{13}$H$_9$Cl$_2$N$_5$·HCl) C, H, N.

5-(2,3-Dichlorophenyl)-1-[(2-methylpyridin-3methyl)methyl]-1*H*-tetrazole hydrochloride (15f): ^{1}H NMR (DMSO-d_6) δ 8.60 (dd, J = 1.7, 5.3 Hz, 1H), 7.95 (dd, J = 1.7, 7.8 Hz, 1H), 7.70–7.67 (m, 1H), 7.70 (dd, J = 1.7, 7.8 Hz, 1H), 7.59 (t, J = 8.0 Hz, 1H), 7.49 (dd, J = 5.4, 7.6 Hz, 1H), 5.77 (s, 2H), 2.47 (s, 3H); MS (ESI$^+$) m/z 321 (M + H)$^+$. Anal. (C$_{14}$H$_{11}$Cl$_2$N$_5$·HCl) C, H, N.

3-{2-[5-(2,3-Dichlorophenyl)tetrazol-1-yl]ethyl}pyridine hydrochloride (15g): ^{1}H NMR (DMSO-d_6) δ 8.70 (m, 2H), 8.22 (d, J = 8.5 Hz, 1H), 7.87 (dd, J = 1.4, 7.1 Hz, 1H), 7.80 (m, 2H), 7.55 (t, J = 7.8 Hz, 1H), 5.20 (t, J = 6.8 Hz, 2H), 3.40 (t, J = 6.8 Hz, 2H); MS (ESI$^+$) m/z 321 (M + H)$^+$. Anal. (C$_{14}$H$_{11}$Cl$_2$N$_5$·HCl) C, H, N.

5-(2,3-Dichlorophenyl)-1-(2,4-dimethylthiazol-5-ylmethyl)-1*H*-tetrazole (15h): mp 174–175 °C; ^{1}H NMR (DMSO-d_6) δ 7.98 (dd, J = 3.1, 6.8 Hz, 1H), 7.63 (dd, J = 4.5, 7.6 Hz, 1H), 7.61 (t, J = 7.5 Hz, 1H), 5.73 (s, 2H), 2.51 (s, 3H), 2.00 (s, 3H); MS (ESI$^+$) m/z 341 (M + H)$^+$. Anal. (C$_{13}$H$_{11}$Cl$_2$N$_5$S) C, H, N.

5-(2,3-Dichlorophenyl)-1-(3,5-dimethylisoxazol-4-ylmethyl)-1*H*-tetrazole (15i): mp 176–178 °C; ^{1}H NMR (DMSO-d_6) δ 7.96 (dd, J = 1.7, 7.8 Hz, 1H), 7.70 (dd, J = 1.7, 7.5 Hz, 1H), 7.62 (t, J = 7.8 Hz, 1H), 5.44 (s, 2H), 2.04 (s, 3H), 1.96 (s, 3H); MS (ESI$^+$) m/z 325 (M + H)$^+$. Anal. (C$_{13}$H$_{11}$Cl$_2$N$_5$O) C, H, N.

3-(5-Phenyltetrazol-1-ylmethyl)pyridine (16a): ^{1}H NMR (DMSO-d_6) δ 8.52 (dd, J = 4.7, 1.4 Hz, 1H), 8.44 (d, J = 2.4 Hz, 1H), 7.75–7.78 (m, 2H), 7.56–7.68 (m, 4H), 7.38 (dd, J = 8.0, 4.9 Hz, 1H), 5.85 (s, 2H); MS (ESI$^+$) m/z 237 (M + H)$^+$. Anal. (C$_{13}$H$_{11}$N$_5$) C, H, N.

3-[5-(2-Chlorophenyl)tetrazol-1-ylmethyl]pyridine hydrochloride (16b): ^{1}H NMR (DMSO-d_6) δ 8.67 (dd, J = 5.1, 1.4 Hz, 1H), 8.53 (d, J = 2.0 Hz, 1H), 7.90 (dt, J = 8.1, 1.7 Hz, 1H), 7.72–7.54 (m, 5H), 6.88 (br s, 1H, HCl), 5.71 (s, 2H); MS (DCI/NH$_3$) m/z 272 (M + H)$^+$. Anal. (C$_{13}$H$_{10}$ClN$_5$·HCl) C, H, N.

3-[5-(3-Chlorophenyl)tetrazol-1-ylmethyl]pyridine (16c): ^{1}H NMR (DMSO-d_6) δ 8.82 (dd, J = 4.8, 1.7 Hz, 1H), 8.44 (d, J = 2.0 Hz, 1H), 7.84 (dd, J = 2.0, 1.8 Hz, 1H), 7.72–7.74 (m, 1H), 7.69–7.71 (m, 1H), 7.63 (d, J = 7.8 Hz, 1H), 7.55–7.60 (m, 1H), 7.37 (dd, J = 7.8, 4.7 Hz, 1H), 5.85 (s, 2H); MS (DCI/NH$_3$) m/z 272 (M + H)$^+$. Anal. (C$_{13}$H$_{10}$ClN$_5$) C, H, N.

3-[5-(2,5-Dichlorophenyl)tetrazol-1-ylmethyl]pyridine (16d): mp 200–201 °C; ^{1}H NMR (DMSO-d_6) δ 8.64 (dd, J = 1.7, 5.1 Hz, 1H), 8.51 (d, 1H, J = 1.7 Hz, 1H), 7.89 (d, J = 2.7 Hz, 1H), 7.82 (m, 1H), 7.79 (dd, J = 2.7, 8.8 Hz, 1H), 7.74 (t, J = 9.2 Hz, 1H), 7.58 (dd, J = 5.1, 8.1 Hz, 1H), 5.71 (s, 2H); MS (ESI$^+$) m/z 307 (M + H)$^+$. Anal. (C$_{13}$H$_{10}$Cl$_3$N$_5$) C, H, N.

3-[5-(3,4-Dichlorophenyl)tetrazol-1-ylmethyl]pyridine (16e): mp 166–168 °C; ^{1}H NMR (DMSO-d_6) δ 8.53 (dd, J = 1.7, 4.8 Hz, 1H), 8.45 (d, J = 2.0 Hz, 1H), 8.05 (d, J = 2.0 Hz, 1H), 7.88 (d, J = 8.5 Hz, 1H), 7.75 (dd, J = 2.0, 8.5 Hz, 1H), 7.58 (td, J = 1.7, 7.8 Hz, 1H), 7.38 (ddd, J = 1.0, 4.7, 8.1 Hz, 1H), 5.84 (s, 2H); MS (ESI$^+$) m/z 307 (M + H)$^+$.

5-(2,3-Dimethylphenyl)-1-(2-methylbenzyl)-1*H*-tetrazole (16f): ^{1}H NMR (CDCl$_3$) δ 7.32 (d, J = 7.4 Hz, 1H), 7.21–7.15 (m, 2H), 7.10 (d, J = 7.4 Hz, 1H), 7.04–6.97 (m, 2H), 6.68 (d, J = 7.8 Hz, 1H), 5.38 (s, 2H), 2.27 (s, 3H), 2.12 (s, 3H), 1.76 (s, 3H); MS (ESI$^+$) m/z 279 (M + H)$^+$. Anal. (C$_{17}$H$_{18}$N$_4$) C, H, N.

1-(2-Chlorobenzyl)-5-(2,3-dimethoxyphenyl)-1*H*-tetrazole (16g): ^{1}H NMR (DMSO-d_6) δ 7.46–7.16 (m, 6H), 7.02 (dd, J = 7.5, 1.4 Hz, 1H), 5.59 (s, 2H), 3.88 (s, 3H), 3.60 (s, 3H); MS (DCI/NH$_3$) m/z 331 (M + H)$^+$. Anal. (C$_{16}$H$_{15}$ClN$_4$O$_2$) C, H, N.

4-(1-Benzyl-1*H*-tetrazol-5-yl)pyridine (16h): ^{1}H NMR (DMSO-d_6) δ 8.76–8.78 (m, 2H), 7.97–7.99 (m, 2H), 7.36–7.45 (m, 5H), 6.05 (s, 2H); MS (ESI$^+$) m/z 279 (M + H)$^+$. Anal. (C$_{17}$H$_{18}$N$_4$) C, H, N.

1-Benzyl-5-(2,3-dichloro-4-pyrrolidin-1-yl-phenyl)-1*H*-tetrazole (16k): ^{1}H NMR (CDCl$_3$) δ 7.28–7.24 (m, 3H), 7.07–7.04 (m, 2H), 6.94 (d, J = 8.8 Hz, 1H), 6.74 (d, J = 8.8 Hz, 1H), 5.43 (s, 2H), 3.55–3.50 (m, 4H), 2.02–1.98 (m, 4H); MS (ESI$^+$) m/z 374 (M + H)$^+$. Anal. (C$_{18}$H$_{17}$Cl$_2$N$_5$) C, H, N.

3-[5-(3-Fluoro-2-trifluoromethylphenyl)tetrazol-1-ylmethyl]pyridine (16l): ^{1}H NMR (CDCl$_3$) δ 8.58 (d, J = 3.7 Hz, 1H), 8.25 (br s, 1H), 7.69–7.63 (m, 1H) 7.56–7.46, m 2H), 7.31–7.26 (m, 1H), 6.97 (d, J = 7.8 Hz, 1H), 5.41 (s, 2H); MS (ESI$^+$) m/z 324 (M + H)$^+$. Anal. (C$_{14}$H$_9$F$_4$N$_5$) C, H, N.

3-[5-(2-Chloro-3-trifluoromethylphenyl)tetrazol-1-ylmethyl]pyridine hydrochloride (16m): ^{1}H NMR (DMSO-d_6) δ 8.66 (d, J = 5.1 Hz, 1H), 8.53 (d, J = 1.4 Hz, 1H), 8.17 (dd, J = 7.8, 1.4 Hz, 1H), 7.89 (d, J = 7.8 Hz, 1H), 7.80 (dd, J = 7.8, 7.7 Hz, 1H), 7.61 (dd, J = 8.1, 5.1 Hz, 1H), 5.74 (s, 2H), 5.70 (br s, 1H); MS (ESI$^+$) m/z 340 (M + H)$^+$. Anal. (C$_{14}$H$_9$ClF$_4$N$_5$·HCl) C, H, N.

3-[5-(2-Fluoro-3-trifluoromethylphenyl)tetrazol-1-ylmethyl]pyridine (16n): ^{1}H NMR (CDCl$_3$) δ 8.57 (br s, 1H), 8.39 (br s, 1H), 7.90–7.85 (m, 1H), 7.73–7.68 (m, 1H), 7.56 (d, J = 7.8 Hz, 1H), 7.46–7.41 (m, 1H), 7.30 (br s, 1H), 5.61 (s, 2H); MS (ESI$^+$) m/z 324 (M + H)$^+$. Anal. (C$_{14}$H$_9$F$_4$N$_5$) C, H, N.

3-[5-(2,3,4-Trichlorophenyl)tetrazol-1-ylmethyl]pyridine (16p): ^{1}H NMR (CDCl$_3$) δ 8.59 (br s, 1H), 8.32 (br s, 1H), 7.54–7.50 (m, 2H), 7.30–7.26 (m, 1H), 7.10 (d, 1H), 5.48 (s, 2H); MS (ESI$^+$) m/z 340 (M + H)$^+$. Anal. (C$_{13}$H$_8$Cl$_3$N$_5$) C, H, N.

Representative Procedure for Conversion of Amides to Tetrazoles (Route 2, Step d). 3-[5-(2,3-Dichloro-4-fluorophenyl)-tetrazol-1-ylmethyl]pyridine. To an oven-dried, N$_2$-purged, 25-mL, round-bottomed flask containing a magnetic stir bar were added solid 2,3-dichloro-4-fluoro-*N*-pyridin-3-ylmethylbenzamide (299 mg, 1.00 mmol) and triphenylphosphine (525 mg, 2.00 mmol). The flask was sealed with a septum and purged with N$_2$ atmosphere. Anhydrous THF (5 mL) was added via syringe to form a pale yellow solution. Diisopropyl azodicarboxylate (387 μL, 2.00 mmol) was added via syringe to form a light brown solution. Azidotrimethylsilane (265 μL, 2.00 mmol) was added via syringe, and a thick, white precipitate formed immediately. The reaction was stirred at room temperature for 24 h, during which time the progress of the reaction was monitored by TLC (silica gel, 40% isopropyl alcohol, 60% hexanes; amide R_f = 0.4, product R_f = 0.3). Water (10 mL) was added to quench the reaction and a brown solution formed. The reaction was transferred to a 125-mL separatory funnel and extracted with CH$_2$Cl$_2$ (3 × 10 mL). The combined organic extracts were dried over MgSO$_4$, filtered, and concentrated by rotary evaporator to give a brown oil. The product was obtained by flash chromatography using TLC conditions to give 46 mg (76%) of a white powder.

5-(1-Benzyl-1*H*-tetrazol-5-yl)quinoline (16i): ^{1}H NMR (DMSO-d_6) δ 8.98 (dd, J = 4.2, 1.5 Hz, 1H), 8.28 (d, J = 8.5 Hz, 1H), 7.96–7.84 (m, 3H), 7.52 (dd, J = 8.6, 4.2 Hz, 1H), 7.20–7.15 (m, 3H), 6.97–6.93 (m, 2H), 5.63 (s, 2H); MS (ESI$^+$) m/z 288 (M + H)$^+$. Anal. (C$_{17}$H$_{13}$N$_5$) C, H, N.

8-(1-Benzyl-1*H*-tetrazol-5-yl)quinoline (16j): ^{1}H NMR (DMSO-d_6) δ 8.93 (dd, J = 4.2, 1.9 Hz, 1H), 8.57 (dd, J = 8.1, 1.7 Hz, 1H), 8.29 (dd, J = 8.1, 1.4 Hz, 1H), 7.91 (dd, J = 7.3, 1.5 Hz, 1H), 7.75 (dd, J = 7.5, 7.4 Hz, 1H), 7.70 (dd, J = 8.3, 4.2 Hz, 1H), 7.21–7.15 (m, 3H), 6.91–6.88 (m, 2H), 5.52 (s, 2H); LCMS (ESI$^+$) m/z 288 (M + H)$^+$. Anal.(C$_{17}$H$_{13}$N$_5$) C, H, N.

3-[5-(2,3-Dichloro-4-fluorophenyl)tetrazol-1-ylmethyl]pyridine hydrochloride (16o): ^{1}H NMR (DMSO-d_6) δ 8.66(dd, J = 5.1, 1.4 Hz, 1H), 8.54 (d, J = 1.7 Hz, 1H), 7.87 (d, J = 7.8 Hz, 1H), 7.81–7.70 (m, 2H), 7.60 (dd, J = 8.1, 5.1 Hz, 1H), 5.71 (s, 2H); MS (ESI$^+$) m/z 324 (M + H)$^+$. Anal. Calcd for C$_{13}$H$_9$Cl$_3$FN$_5$: C, 43.30; H, 2.52; N, 19.42. Found: C, 42.66; H, 2.22; N, 19.06.

Representative Procedure for Conversion of Thioamides to Tetrazoles (Route 3, Step g). 3-[1-(2,3-Dichlorophenyl)-1*H*-tetrazol-5-ylmethyl]pyridine (17a). To an oven-dried, N$_2$-purged, 25-mL, round-bottomed flask containing a magnetic stir bar was added *N*-(2,3-dichlorophenyl)-2-pyridin-3-ylthioacetamide (208 mg, 0.700 mmol). Anhydrous tetrahydrofuran (7 mL) was added via syringe to form a pale yellow solution. The flask was cooled to 0

°C in an ice bath. Solid mercury(II) acetate (446 mg, 1.40 mmol) was added to form a slurry. The flask was sealed with a septum and purged with N$_2$ atmosphere. Azidotrimethylsilane (806 mg, 921 mL, 7.00 mmol) was added via syringe. The yellow slurry was stirred at 0 °C for 1 h. Saturated ammonium chloride solution (10 mL) was added and the mixture was transferred to a 125-mL separatory funnel. The emulsion was extracted with dichloromethane (3 × 10 mL). The combined organic extracts were dried over sodium sulfate, filtered, and concentrated by rotary evaporator. The product was purified by flash chromatography (silica gel/ethyl acetate, product $R_f = 0.4$) to give 203 mg (95%) of a white powder.

3-[1-(2,3-Dichlorophenyl)-1H-tetrazol-5-ylmethyl]pyridine (17a): ^{1}H NMR (DMSO-d_6) δ 8.43 (dd, $J = 4.7, 1.7$ Hz, 1H), 8.27 (d, $J = 2.4$ Hz, 1H), 7.99 (dd, $J = 8.1, 1.4$ Hz, 1H), 7.83 (dd, $J = 8.0$ 1.5 Hz, 1H), 7.65 (dd, $J = 8.1, 8.0$ Hz, 1H), 7.51–7.55 (m, 1H), 7.28 (dd, $J = 7.3, 5.3$ Hz, 1H), 4.29 (s, 2H); MS (ESI$^+$) m/z 306 (M + H)$^+$. Anal.(C$_{13}$H$_9$Cl$_2$N$_5$) C, H, N.

3-[1-(2,3-Dichloro-4-fluorophenyl)-1H-tetrazol-5-ylmethyl]pyridine Hydrochloride (17b). The free base was prepared according to the procedure for route 3, step g. The hydrochloride salt was prepared by treatment of the free base with etheric HCl: ^{1}H NMR (DMSO-d_6) δ 8.67 (d, $J = 3.7$ Hz, 1H), 8.59 (d, $J = 1.7$ Hz, 1H), 8.04 (d, $J = 8.1$ Hz, 1H), 7.97 (dd, $J = 9.0, 5.3$ Hz, 1H), 7.82 (dd, $J = 8.8$ Hz, 1H), 7.68 (dd, $J = 8.0, 5.3$ Hz, 1H), 4.40 (s, 2H); MS (ESI$^+$) m/z 324 (M + H)$^+$. Anal.(C$_{13}$H$_9$Cl$_3$FN$_5$) C, H, N.

3-[1-(2-Chloro-3-trifluoromethylphenyl)-1H-tetrazol-5-yl-methyl]pyridine Hydrochloride (17c). The free base was prepared according to the procedure for route 3, step g. The hydrochloride salt was prepared by treatment of the free base with etheric HCl: ^{1}H NMR (DMSO-d_6) δ 8.63 (dd, $J = 5.4, 1.4$ Hz, 1H), 8.53 (d, $J = 2.0$ Hz, 1H), 8.23–8.19 (m, 2H), 7.97 (d, $J = 7.8$ Hz, 1H), 7.88 (dd, $J = 7.8$ Hz, 1H), 7.62 (dd, $J = 8.0, 5.3$ Hz, 1H), 4.42 (s, 2H); MS (ESI$^+$) m/z 339.9 (M + H)$^+$. Anal.(C$_{14}$H$_{10}$Cl$_2$F$_3$N$_5$) C, H, N.

3-[1-(2-Chloro-4-fluoro-3-trifluoromethylphenyl)-1H-tetrazol-5-ylmethyl]pyridine Hydrochloride (17d). The free base was prepared according to the procedure for route 3, step g. The hydrochloride salt was prepared by treatment of the free base with etheric HCl: ^{1}H NMR (DMSO-d_6) δ 8.48 (dd, $J = 4.7, 1.4$ Hz, 1H), 8.36 (d, $J = 2.0$ Hz, 1H), 8.28 (dd, $J = 8.8, 5.1$ Hz, 1H), 7.87 (dd, $J = 10.5, 10.0$ Hz, 1H), 7.66 (d, $J = 7.8$ Hz, 1H), 7.38 (dd, $J = 7.6, 4.9$ Hz, 1H), 4.33 (s, 2H); MS (ESI$^+$) m/z 358 (M + H)$^+$.

Electrophysiology. Whole-cell patch-clamp recordings were obtained from stably transfected hP2X$_7$ 1321N1 cells plated on polyethylenimine-coated coverslips grown to approximately 50% confluence. Currents were recorded using an Axopatch 200B amplifier (Axon Instruments, Molecular Devices Corp., Union City, CA) and digitized at 3 kHz for acquisition. The chamber containing the cells was continuously perfused by an extracellular recording solution (pH 7.4, 320 mosM) consisting of 147 mM NaCl, 2 mM KCl, 2 mM CaCl$_2$, 1 mM MgCl$_2$, 10 mM Hepes, and 13 mM glucose. Patch electrodes were pulled from borosilicate glass and fire-polished to 3–6 MΩ tip resistance. The intracellular solution (pH 7.3, 300 mosM) contained 145 mM NaF, 10 mM EGTA, and 10 mM Hepes). All cells were voltage-clamped at −60 mV, and series resistance was compensated 85–90%.

Cells were constantly perfused with extracellular solution at a rate of 0.5 mL/min in the recording chamber. Agonist was delivered to individual cells using a piezoelectric-driven rapid application system (Burleigh Instruments, Fishers, NY). Extracellular solution perfused the cell from one barrel of a glass θ tube positioned 100 μm away. Agonist solution perfused the other barrel, and was applied by rapidly moving the solution interface across the cell. Agonist applications were approximately 2 s in duration and were given in approximately 1-min intervals. Antagonist was preapplied using the extracellular solution barrel of the θ tube for at least 30 s before coapplication with agonist through the other barrel. Current responses were acquired and analyzed using pClamp software (Axon Instruments, Molecular Devices Corp., Union Cjity, CA). Current amplitudes were measured at the end of the agonist application pulse when a current plateau was achieved. All reagents were purchased from Sigma Chemical (St Louis, MO).

Supporting Information Available: Elemental analysis data and representative synthetic procedures and characterization data for intermediates and immediate precursors to tetrazoles. This material is available free of charge via the Internet at http://pubs.acs.org.

References

(1) North, R. A.; Barnard, E. A. Nucleotid receptors. *Curr. Opin. Neurobiol*. **1997**, *7*, 346−357.

(2) Ralevic, V.; Burnstock, G. Receptors for purines and pyrimidines. *Pharmacol. Rev.* **1998**, *50*, 413−492.

(3) Jacobsen, K. A.; Jarvis, M. F.; Williams, M. Purine and pyrimidine (P2) receptors as drug targets. *J. Med. Chem.* **2002**, *45*, 4057−4093.

(4) North, R. A. Molecular physiology of P2X receptors. *Physiol. Rev.* **2002**, *82*, 1013−1067.

(5) Burnstock, G.; King, B. F. Numbering of cloned P2 receptors. *Drug Dev. Res.* **1996**, *38*, 67−71.

(6) Surprenant A.; Rassendren, F.; Kawashima, E.; North, R. A.; Buell, G. The cytolytic P2Z receptor for extracellular ATP identified as a P2X (P2X7) receptor. *Science* **1996**, *272*, 735−738.

(7) El-Moatassim, C.; Dubyak, G. R. A novel pathway for the activation of phospholipase D by P2Z purinergic receptors in BAC1.2F5 macrophages. *J. Biol. Chem.* **1992**, *267*, 23664−23673.

(8) Falzoni, S.; Munerati, M.; Ferrari, D.; Spisani, S.; Moretti, S.; Di Virgilio, F. The purinergic P2Z receptor of human macrophage cells. Characterization and possible physiological roles. *J. Clin. Invest.* **1995**, *95*, 1207−1216.

(9) Rassendren, F.; Buell, G. N.; Virginio C.; Collo, G.; North, R. A.; Surprenant, A. The permeabilizing ATP receptor, P2X7. *J. Biol Chem.* **1997**, *272*, 5482−6486.

(10) Ferrari, D.; Villalba, M.; Chiozzi, P.; Falzoni, S.; Ricciardi-Castagnoli, P.; DiVirgilio, F. Mouse microglia cells express a plasma membrane pore gated by extracellular ATP. *J. Immunol.* **1996**, *156*, 1531−1539.

(11) (a) Irnich, D.; Burgstahler, R. Grafe, P. P2 nucleotide receptors in peripheral nerve trunk. *Drug Dev. Res.* **2001**, *52*, 83−88. (b) Ballerini, P.; Rathbone, M. P.; Di Iorio, P.; Renzetti, A.; Giuliani, P.; D'Alimonte, I.; Trubiani, O.; Caciagli, F.; Ciccarelli, R. Rat astroglial P2Z (P2X7) receptors regulate intracellular calcium and purine release. *Neuroreport* **1996**, *7*, 2533−2537.

(12) (a) Deuchars, S. A.; Atkinson, L.; Brooke, R. E.; Musa, H.; Milligan, C. J.Batten, T. F. C.; Buckley, N. J.; Parson, S. H.; Deuchars, J. Neuronal P2 × 7 receptors are targeted to presynaptic terminals in the central and peripheral nervous system. *J. Neurosci.* **2001**, *21*, 7143−7152. (b) Sim, J. A.; Young, M. T.; Sung, H.-Y.; North, R. A.; Surprenant, A. Reanalysis of P2X7 Receptor Expression in Rodent Brain. *J. Neurosci.* **2004**, *24*, 6307−6314.

(13) Buisman, H. P.; Steinberg, T. H.; Fischbarg, J.; Silverstein, S. C.; Vogelzang, S. A.; Ince, C.; Ypey, D. L.; Leijh, P. C. Extracellular ATP induces a large nonselective conductance in macrophage plasma membranes. *Proc. Natl. Acad. Sci. U.S.A.* **1988**, *85*, 7988−7992.

(14) Kahlenberg, J. M.; Dubyak, G. W. Mechanisms of caspase-1 activation by P2X7 receptor-mediated K$^+$ release. *Am. J. Cell Physiol.* **2004**, *286*, C1100−C1108.

(15) Perregaux, D.; Gabel, C. A. Interleukin-1 β maturation and release in response to ATP and nigericin. Evidence that potassium depletion mediated by these agents is a necessary and common feature of their activity. *J. Biol. Chem.* **1994**, *269*, 15195−15203.

(16) Walev, I.; Klein, J.; Husmann, M.; Valeva, A.; Strauch, S.; Wittz, H.; Weichel, O.; Bhakdi, S. Potassium inhibited processing of IL-1β in human monocytes. *EMBO J.* **1995**, *14*, 1607−1614.

(17) Donnelly-Roberts, D. L.; Namovic, M.; Faltynek, C. R.; Jarvis, M. F. Mitogen-activated protein kinase and caspase signaling pathways are required for p2X7 receptor (P2X7R)-induced pore formation in Human THP-1 cells. *J. Pharmacol. Exp. Ther.* **2004**, *308*, 1053−1061.

(18) (a) Papp, L.; Vizi, E. S.; Sperlágh, B. Lack of ATP-evoked GABA and glutamate release in the hippocampus of P2X7 receptor −/− mice. *Neuroreport* **2004**, *15*, 2387−2391. (b) Duan, S.; Anderson, C. M.; Keung, E. C.; Chen, Y.; Chen, Y.; Swanson, R. A. P2X7 Receptor-Mediated Release of Excitatory Amino Acids from Astrocytes. *J. Neurosci.* **2003**, *23*, 1320−1328.

(19) (a) DiVirgilio, F.; Vishwanath, V.; Ferrari, D. On the Role of the P2X7 Receptor in the Immune System. *Handbook Exp. Pharmacol.* **2001**, *151*, 355−374. (b) DiVirgilio, F.; Falzoni, S.; Mutini, C.; Sanz, J. M.; Chiozzi, P. Purinergic P2X7 receptor: A pivotal role in inflammation and immunomodulation. *Drug. Dev. Res.* **1998**, *45*, 207−213.

(20) (a) LeFeuvre, R. A.; Brough, D.; Touzani, O.; Rothwell, N. J. Role of P2X7 receptors in ischemic and excitotoxic brain injury in vivo. *J. Cerebr. Blood Flow Metab.* **2003**, *23*, 381−384. (b) LeFeuvre, R.; Brough, D.; Rothwell, N. Extracellular ATP and P2X7 receptors in neurodegeneration. *Eur. J. Pharmacol.* **2002**, *447*, 261−269. (c)

Rampe, D.; Wang, L.; Ringheim, G. E. P2X7 receptor modulation of β-amyloid- and LPS-induced cytokine secretion from human macrophages and microglia. *J. Neuroimmunol.* **2004**, *147*, 56−61. (d) Wang, X.; Arcuino, G.; Takano, T.; Lin, J.; Peng, W. G.; Wan, P.; Li, P.; Xu, Q.; Liu, Q. S.; Goldman, S. A.; Nedergaard, M. P2X7 receptor inhibition improves recovery after spinal cord injury. *Nature Med.* **2004**, *10*, 821−827.

(21) (a) Raghavendra, V.; DeLeo, J. A. The role of astrocytes and microglia in persistent pain. *Adv. Mol. Cell Biol.* **2004**, *31*, 951−966. (b) Milligan, E. D.; Maier, S. F.; Watkins, L. R. Review: Neuronal−glial interactions in central sensitization. *Sem. Pain Med.* **2003**, *1*, 171−183.

(22) Woolf, C. J.; Allchorne, A.; Safieh-Garabedien, B.; Poole, S. Cytokines, nerve growth factor and inflammatory hyperalgesia: The contribution of tumor necrosis factor alpha. *Br. J. Pharmacol.* **1997**, *121*, 417−424.

(23) DeLeo, J. A.; Yezierski, R. P. The role of neuroinflammation and neuroimmune activation in persistent pain. *Pain* **2001**, *90*, 1−6.

(24) Hanani, M.; Huang, T. Y.; Cherkas, P. S.; Ledda, M.; Pannese, E. Glial cell plasticity in sensory ganglia induced by nerve damage. *Neuroscience* **2002**, *114*, 279−283.

(25) Costigan, M.; Woolf, C. J. Pain: Molecular mechanisms. *J. Pain* **2000**, *1*, 35−44.

(26) (a) Labasi, J. M.; Petrushova, N.; Donovan, C.; McCurdy, S.; Lira, P.; Payette, M. M.; Brissette, W.; Wicks, J. R.; Audoly, L.; Gabel, C. A. Absence of the P2X7 receptor alters leukocyte function and attenuates an inflammatory response. *J. Immunol.* **2002**, *168*, 6436−6445. (b) Chessell, I. P.; Hatcher, J. P.; Bountra, C.; Michel, A. D.; Hughes, J. P.; Green, P.; Egerton, J.; Murfin, M.; Richardson, J.; Peck, W. L.; Grahames, C. B. A.; Casula, M. A.; Yiangou, Y.; Birch, R.; Anand, P.; Buell, G. N. *Pain* **2005**, *114*, 386-396.

(27) Dell'Antonio, G.; Quattrini, A.; Cin, E. D.; Fulgenzi, A.; Ferrero, M. E. Relief of inflammatory pain in rats by local use of the selective P2X7 ATP receptor inhibitor, oxidized ATP. *Arthritis Rheum.* **2002**, *46*, 3378−3385.

(28) Gargett, C. E.; Wiley, J. S. The isoquinoline derivative KN-62 a potent antagonist of the P2Z-receptor of human lymphocytes. *Br. J. Pharmacol.* **1997**, *120*, 1483−1490.

(29) (a) KN62 analogues: Baraldi, P. G.; Romagnoli, R.; Tabrizi, M. A.; Falzoni, S.; Di Virgilio, F. Synthesis of Conformationally constrained analgues of KN62, a potent antagonist of the P2X7-receptor. *Bioorg. Med. Chem. Lett.* **2000**, *10*, 681−684. (b) Ravi, R. G.; Kertesy, S. B.; Dubyak, G. R.; Jacobsen, K. A. Potent P2X7 receptor antagonists: Tyrosyl derivatives synthesized using a sequential parallel synthetic approach. *Drug Dev. Res.* **2001**, *54*, 75−87. (c) Chen, W.; Ravi, R. G.; Kertesy, S. B.; Dubyak, G. R.; Jacobsen, K. A. Functionalized congeners of tyrosine-based P2X7 receptor antagonists: Probing multiple sites for linking and dimerization. *Bioconjugate Chem.* **2002**, *13*, 1100−1111. (d) Baraldi, P. G.; del Carmen

Nunez, M.; Morelli, A.; Falzoni, S.; DiVirgilio, F.; Romagnoli, R. Synthesis and biological activity of N-arylpiperazine-modified analogues of KN-62, a potent antagonist of the purinergic P2X7 receptor. *J. Med. Chem.* **2003**, *46*, 1318−1329.

(30) Alcaraz, L.; Baxter, A.; Bent, J.; Bowers, K.; Braddock, M.; Cladingboel, D.; Donald, D.; Fagura, M.; Furber, M.; Laurent, C.; Lawson, M.; Mortimer, M.; McCormick, M.; Roberts, N.; Robertson, M. Novel P2X7 receptor antagonists. *Bioorg. Med. Chem. Lett.* **2003**, *8*, 4043−4046.

(31) Baxter, A.; Bent, J.; Bowers, K.; Braddock, M.; Brough, S.; Fagura, M.; Lawson, M.; McInally, T.; Mortimer, M.; Robertson, M.; weaver, R.; Webborn, P. Hit-to-lead studies: The discovery of potent adamantane amide P2X7 receptor antagonists. *Bioorg. Med. Chem. Lett.* **2003**, *8*, 4047−4050.

(32) Perez-Medrano, A.; Donnelly-Roberts, D. L.; Faltynek, C. R.; Honore, P.; Jarvis, M. F.; Peddi, S.; Wang, Y.; Carroll, W. A. Discovery and biological evaluation of novel cyanoguanidine P2X7 antagonists for the treatment of neuropathic pain. *J. Med. Chem.* Submitted for publication.

(33) Huff, B. E.; Staszak, M. A. A new method for the preparation of tetrazoles from nitriles using trimethylsilylazide/trimethylaluminum. *Tetrahedron Lett.* **1993**, *34*, 8011−8014.

(34) The regiochemistry of the 1,5- and 2,5-substituted products **8a** and **8b** was determined from the NOE effect observed for the 1,5-isomer between the benzylic protons and the ortho hydrogen on the adjacent group Ar. No NOE effect was observed for the 2,5-isomer.

(35) Duncia, J. V.; Pierce, M. E.; Santella, J. B., III. Three synthetic routes to a sterically hindered tetrazole. A new one-step mild conversion of an amide into a tetrazole. *J. Org. Chem.* **1991**, *56*, 2395−2400.

(36) Panday, N.; Meyyappan, M.; Vasella, A. A comparison of glucose- and glucosamine-related inhibitors: Probing the interaction of the 2-hydroxy group with retaining β-glucosidases. *Helv. Chim. Acta* **2000**, *83*, 513−538.

(37) Bianchi, B. R.; Lynch, K. J.; Touma, E.; Niforatos, W.; Burgard, E. C.; Alexander, K. M.; Park, H. S.; Yu, H.; Metzger, R.; Kowaluk, E. Pharmacological characterization of recombinant human and rat P2X receptor subtypes. *Eur. J. Pharmacol.* **1999**, *376*, 127−138.

(38) Jarvis, M. F.; Burgard, E. C.; McGaraughty, S.; Honore P.; Lynch, K.; Brennan, T. J.; Subieta, A.; van Biesen, T.; Cartmell, J.; Bianchi, B.; Niforatos, W.; Kage, K.; Yu, H.; Mikusa, J.; Wismer, C. T.; Zhu, C. Z.; Chu, K.; Lee, C.-H.; Stewart, A. O.; Polakowski, J.; Cox, B. F.; Kowaluk, E.; Williams, M.; Sullivan, J.; Faltynek, C. A-317491, a novel potent and selective nonnucleotide antagonist of P2X3 and P2X2/3 receptors, reduces chronic inflammatory and neuropathic pain in the rat. *Proc. Natl. Acad. Sci. U.S.A.* **2002**, *99*, 17179−17184.

(39) In pharmacokinetic studies, compound **15d** was administered at a dose of 10 μmol/kg.